Supporting Information

Elucidating the Li-Ion Battery Performance Benefits Enabled by Multi-functional Separators

Hanshuo Liu,[†] Anjan Banerjee,[‡] Baruch Ziv,[‡] Kristopher J. Harris,[††] Nicholas P. W. Pieczonka,[§] Shalom Luski,[‡] Gianluigi A. Botton,[†] Gillian R. Goward,[††] Doron Aurbach,[‡] and Ion C. Halalay*[§]

[†] Department of Materials Science and Engineering, [††]Department of Chemistry, McMaster University, Hamilton, Ontario L8S4K1, Canada.

[*]Department of Chemistry, Bar-Ilan University, Ramat-Gan 5290002, Israel.

[§] General Motors, Global Research & Development, Warren, MI 48092-2031, USA.

*Corresponding author email: ion.c.halalay@gm.com

Experimental Details

Commercial materials were used throughout the present work without purification or modifications. Tests were performed at room temperature (30°C), unless otherwise specified.

Electrode fabrication. Positive electrodes were prepared with LMO by spreading a slurry comprising a 1:1 w/w mixture of electrode components (85 wt% LMO, 10 wt% Super P Li carbon black conductive filler from IMERYS Ltd., 5 wt% PVdF binder from Solvay) and N-methyl pyrrolidone (Sigma Aldrich) as dispersing solvent onto Al current-collectors, using a doctor blade with a 100 µm gap. Graphite negative electrodes were prepared similarly, by doctor-blading a slurry consisting of electrode solids (90 wt% graphite (SMG Hitachi Inc.), 3 wt% carbon black Super P Li (IMERYS Ltd.), 7 wt% PVdF binder (Solvay) and N-methyl pyrrolidone (Sigma Aldrich), onto 10 µm thick Cu foil current collectors. All electrodes were vacuum dried at 120°C for 14 h prior to cell assembly. Active material loadings in the electrodes were ~10.8 mg×cm^{-2} for LMO and ~4.5 mg cm^{-2} for graphite.

Separator fabrication. Two separator membranes with multifunctional material loadings in the approximate ratios 1:4.2 and thickness of 10 and 25 µm, respectively, were fabricated in-house through a phase-inversion technique, with acetone as solvent and water as anti-solvent. Poly(vinylidene fluoride-hexafluoropropylene) (PVdF-HFP) copolymer (Solvay) and a commercial polymeric ion chelating resin consisting of a styrene-divinylbenzene polymer backbone functionalized with disodium iminodiacetate were used, respectively, as matrix and filler. The copolymer to chelating filler mass ratio in the multifunctional

separators was varied in order to provide the mechanical properties needed to maintain the separator integrity during cell assembly and disassembly operations. **Table S1** lists the main characteristics of the multifunctional separators.

Cell assembly. LMO-graphite pouch cells were assembled with the two types of multifunctional separators and commercial PP or PVDF-HFP separators as comparison baselines. All cells were filled with 1 M $LiPF_6$ / EC:DMC (1:1 v/v) electrolyte solution in an Ar-filled glove box with moisture and oxygen levels <1 ppm. The geometric area of the electrodes and separators were 10.5 and 16 cm^2, respectively. The LMO loading for all positive electrodes was 114 mg. Since the thickness of the three trapping separators varied, we used additional baseline polypropylene separators adjacent to the multifunctional separators in order to achieve approximately the same inter-electrode distance. Two and one PP separators were used together with MFS 1-1 and MFS 1-2, respectively. All baseline cells contained two stacked plain separators. The nominal inter-electrode distance was thus 50 μm in all cells, except for 60 μm in the cells with MFS 1-1.

Cell testing. Three formation cycles at C/10 rate were performed at 30°C prior to the galvanostatic cycling tests at 0.2C rate and 55°C for 4 weeks, using an Arbin Model BT2000 multichannel battery cycler. Electrochemical ac impedance spectroscopy (EIS) measurements were done at room temperature on 3-electrode cells with a metallic Li reference electrode, using a Solartron Instruments 1225 HF frequency response analyzer and a Solartron Instruments 1287 EI potentiostat, subsequent to formation and at weekly intervals throughout the high temperature cycling tests. EIS spectra were recorded at open circuit voltage in the discharged state (at ~3 V), with 5 mV excitation amplitude, over the frequency range 100 kHz to 10 mHz, with 10 data points per decade.

Post-disassembly analyses. All cells were immediately disassembled subsequent to the end of each cycling test and associated EOT EIS measurement. The Mn amounts in the separators and the Mn, Li and Na amounts in the negative electrodes were determined by **inductively coupled plasma optical emission spectroscopy** (ICP-OES) using an Ultima 2 instrument from Jobin-Yvon Horiba. Mn ions were eluted with 3 M HCl from the used separators and their concentrations were determined after 100x dilution with deionized doubly distilled (DD-DI) water. The Cu supported graphite negative electrodes were dissolved in aqua regia ($HCl:HNO_3$ = 3:1) and aliquots of the solutions thus obtained were diluted by a factor of 100 with DD-DI water before determining Mn, Li, and Na concentrations. After washing with DMC and drying subsequent to cell disassembly, the morphology of the graphite negative electrodes from the cycled cells was characterized using a FEI Magellan 400 high-resolution SEM. The cross-sections of the cycled graphite anodes were prepared and imaged using a Zeiss NVision 40 dual-beam focused ion beam-scanning electron microscope (FIB-SEM) equipped with a gallium ion beam source and a Schottky Field

Emission Gun (FEG). A tungsten layer was deposited on top of the region of interest, to protect its surface morphology. The total sampling lengths for the FIB cross-sections are 30 μm and 18 μm, respectively for the graphite electrode from cells with plain and MFS 1-1 separators. **MAS-NMR** measurements were carried out under a 20 T applied field with a Bruker HD console. ^{19}F NMR spectra were referenced to liquid $CFCl_3$ at 0 ppm. Due to the extremely long ^{19}F T_1 relaxation time constant for LiF, all spectra were recorded after a partial thermal polarization during a short delay (30 s), following a saturation pulse train. ^{23}Na NMR spectra were reference to 1 M $NaCl_{(aq)}$ and were acquired using selective (solid) 90° pulses. Samples of each separator film were cut into small pieces and packed into 1.9 mm diameter NMR rotors inside an Ar glove box, which were then spun at 12-15 kHz in a pure $N_{2(g)}$ environment. All cycled separators and electrodes from cycled cells were washed with DMC and dried inside a glove box prior to the HR-SEM, FIB-SEM and MAS-NMR measurements. All samples were heat-sealed individually in aluminized pouch cell laminates inside an Ar-filled glove box prior to shipping between laboratories and were handled under strict anaerobic conditions throughout the respective measurements. All samples for HR-SEM, FIB-SEM, and MAS-NMR measurements were heat-sealed individually in aluminized pouch cell laminates inside an Ar-filled glove box prior to shipping between laboratories and were handled under strict anaerobic conditions throughout the respective measurements.

Table S1. Physical properties of the multifunctional separators.

Separator Index	PVdF to Filler Ratio	Thickness, μm	Mass Loading, $mg \times cm^{-2}$	Filler Loading, $mg \times cm^{-2}$
MFS 1-1	1:1	10	0.64	0.32
MFS 1-2	1:2	25	2.00	1.33

Table S2. ICP-OES analysis of separators and graphite electrodes harvested from LMO‖graphite cells with MFS 1-2 and a PVDF-HFP separator after 4 weeks of cycling at 55°C. The graphite electrode from the cell with the plain PVDF-HFP baseline separator has 5.2´ more Mn than the graphite electrode harvested from the cell with MFS 1-2. It is worth noting that: (1) the amount of Mn dissolved from LMO in the cell with MFS 1-2 is 3.5´ smaller than the amount dissolved in the cell with PVdF-HFP separator; (2) the graphite electrode from the cell with MFS 1-2 has 5´ less manganese that the graphite electrode from the cell with the PVDF-HFP separator; (3) there is 5´ more Li in MFS 1-2 than in the PVDF-HFP separator; (4) ~18% of the Na from the cell with MFS 1-2 is found in graphite anode.

		Mn		Na		Li	
Separator	Component	$\mu g/cm^2$	$\mu mol/cm^2$	$\mu g/cm^2$	$\mu mol/cm^2$	$\mu g/cm^2$	$\mu mol/cm^2$
MFS 1-2	Separator	4.46	0.08	80.8	3.5	44.7	6.4
	Graphite Anode	8.44	0.15	17.4	0.76	222	32.0
	TOTAL	**12.90**	**0.23**	**98.1**	**4.26**	**266.7**	**48.4**
PVDF-HFP	Separator	0.39	0.01	N/A	N/A	8.73	1. 3
	Graphite Anode	44.3	0.81	N/A	N/A	283	40.8
	TOTAL	**44.7**	**0.82**	**N/A**	**N/A**	**291.7**	**42.1**

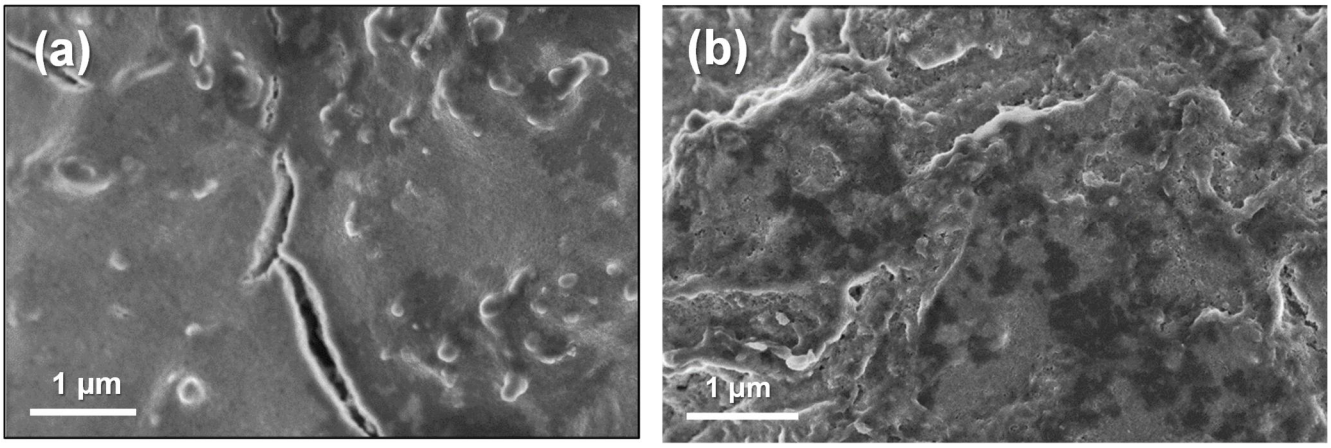

Figure S1. High magnification SEM data for graphite electrode surfaces after 4 weeks of cycling at 0.2C rate and 55ºC in LMO-graphite cells with (**a**) a polypropylene baseline separator or (**b**) MFS 1-1.

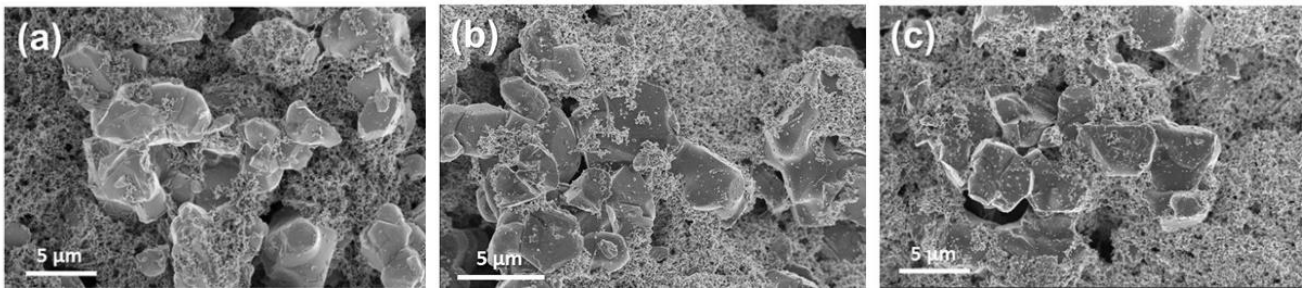

Figure S2. Low magnification HR-SEM images of the surface of LMO electrodes in (**a**) pristine state, as well as after cycling for 4 weeks 0.2C rate and 55ºC in cells with graphite negative electrodes and with (**b**) a plain PP separator and (**c**) separator MFS 1-1. The active material phase is shown as particles in medium grey, the binder plus carbon black mixture as the crinkly, sponge-like structures shown in light grey, and the pores distributed between the particles and binder.

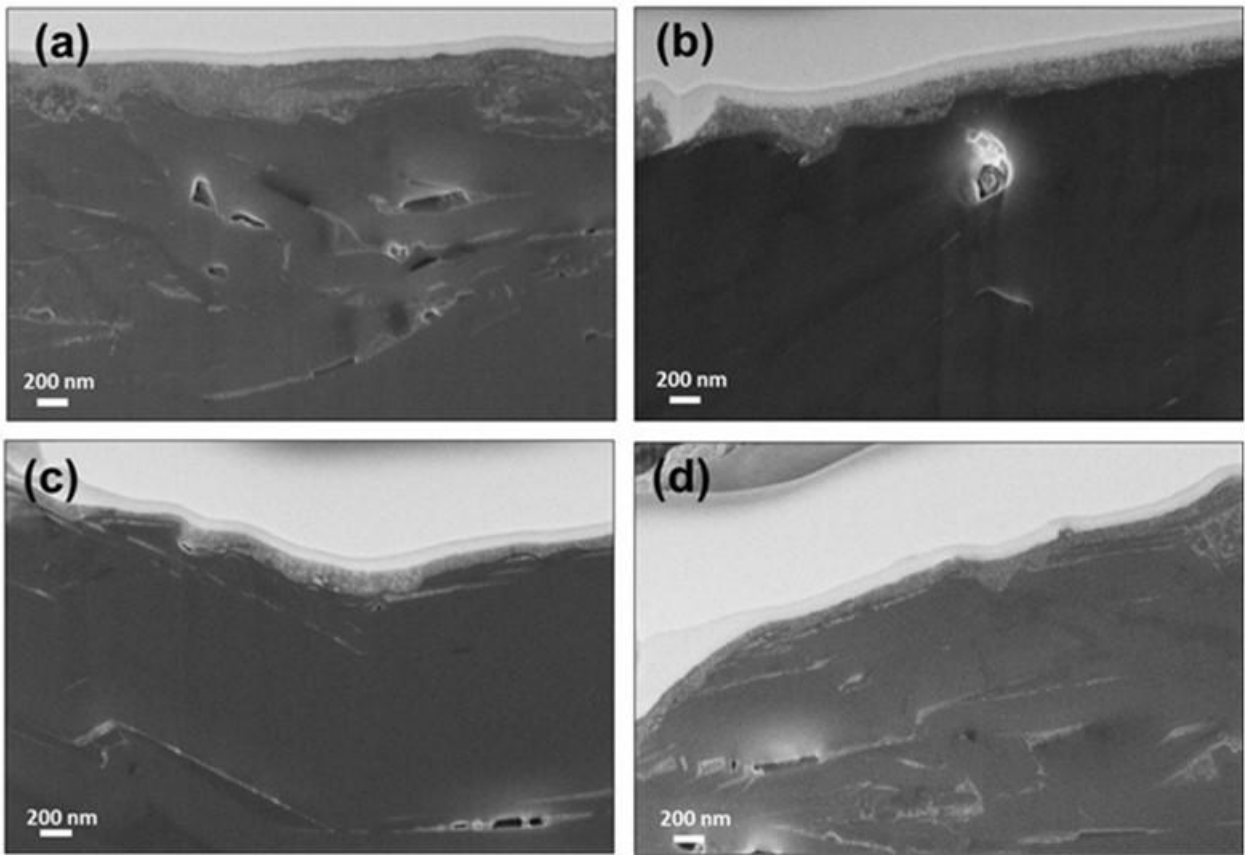

Figure S3. (a) – (d) Representative SEM images recorded for the FIB cross-section of a graphite electrode harvested from an LMO ‖graphite cell with a plain polypropylene separator after 4 weeks of cycling at C/5 rate and 55°C. The white layer at the top of the image is a protective layer of tungsten metal deposited onto the sample surface prior to FIB milling with gallium ions. The SEI is the light gray strip beneath the white strip and the bulk of the electrode seen in darker gray. Besides the SEI with non-uniform thickness at the electrode surface, note that thinner SEI regions inside the pores of the electrode are also visible in the micrographs. The non-uniform nature of the electrode-electrolyte interphase region is clearly visible in panel (a).

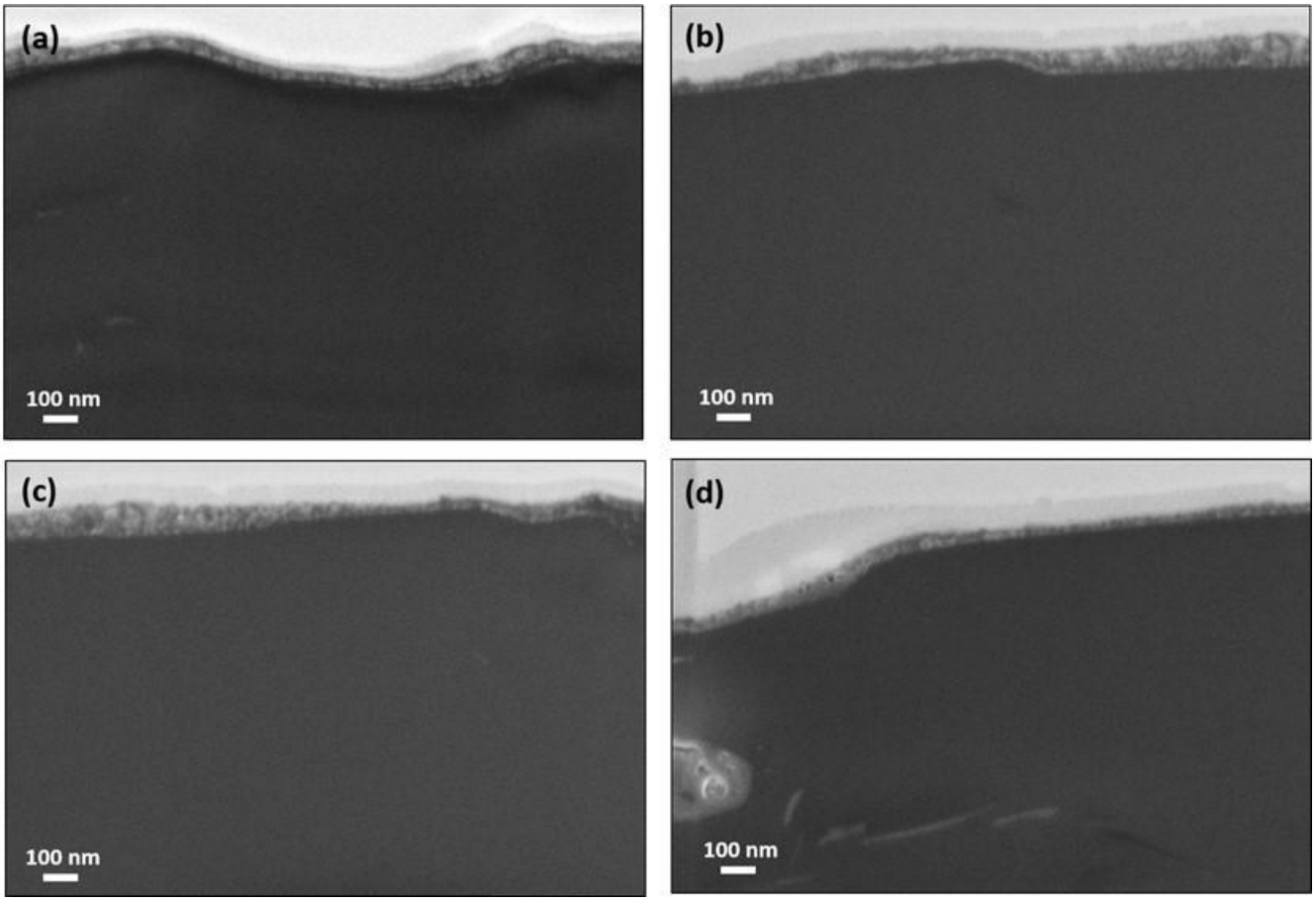

Figure S4. (a) – (d) Representative FIB-SEM images of cross-sections of a graphite electrode from an LMOB‖graphite cell with MFS 1-1 separator after 4 weeks of cycling at C/5 rate and 55°C. The white layer at the top of the image is a protective layer of tungsten metal deposited onto the sample surface prior to FIB milling with gallium ions. The SEI is the light gray strip beneath the white strip and the bulk of the electrode seen in darker gray.

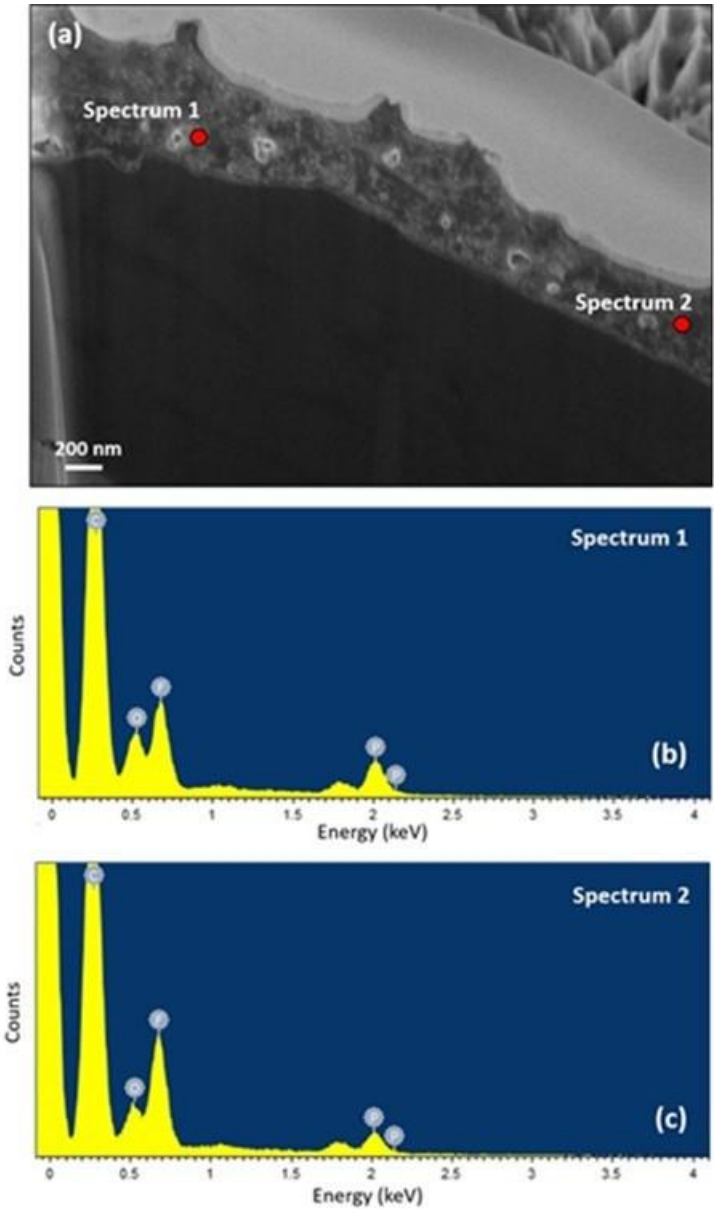

Figure S5. (**a**) FIB-SEM cross-section image of a region from a graphite electrode harvested from a LMO-graphite cell with the MFS 1-1 separator, showing a pocket near the electrode surface that is distinct from most of the SEI on the graphite electrode, consisting of a mixture of SEI, carbon black, and PVdF-HFP binder. (**b**) and (**c**) The EDX spectra recorded in two different areas of the imaged region, marked with red dots in panel (a) indicate inhomogeneity in chemical composition. The ratio of the F to P peaks varies between the two sampled areas. It is clearly distinct in panel (b) from the 6:1 ratio expected from the decomposition of PF_6^- anions. However, in panel (c) the F:P ratio is 5.6, i.e., quite close to 6, which suggests a greater stability of PF_6^- anions in the presence of MFSs.